Use of Stochastic XFEM in the Investigation of Heterogeneity Effects on the Tensile Strength of Intermediate Geotechnical Materials

Mr. Ashley P. Dyson[1] , Mr. Zhan Tang[2], Dr. Ali Tolooiyan[3]

[1]PhD Researcher, Geotechnical and Hydrogeological Engineering Research Group (GHERG), Federation University, email: a.dyson@federation.edu.au

[2]PhD Researcher, Faculty of Science, Monash University, email: zhan.tang@monash.edu

[3]Deputy Director, Geotechnical and Hydrogeological Engineering Research Group (GHERG), Federation University, Northways Rd. Churchill VIC 3842, Australia (Corresponding author), email: ali.tolooiyan@federation.edu.au, tolooiyan@gmail.com

Abstract

The numerical simulation of an Unconfined Expansion Test (UET) is presented with tensile strength fracture criteria assigned by stochastic methods to take into account material heterogeneity. Tests are performed by producing radial cavity expansion models of thinly sliced cylindrical specimens. The introduction of element-wise allocation of fracture parameters generates instances of specimen failure without the requirement of predefined fracture zones, permitting discontinuities to form naturally within zones containing weak strength parameters. The parallel application of an in-house Python scripts and eXtended Finite Element Method (XFEM) facilitates the investigation of heterogeneity effects on the tensile strength of intermediate geotechnical materials.

Keywords:

Intermediate geotechnical material

Fracture mechanics

Stochastic methods

Extended finite element method

Unconfined expansion test

1. Introduction and Background

Conventional numerical modelling methods such as the Finite Element Method (FEM) often perform poorly in approximation of solutions with non-smooth characteristics in the modelling domain, for example near discontinuities, crack initiation/propagation, and singularities. The eXtend Finite Element Method (XFEM) developed by Belytschko and Black [1] is an effective method to simulate discontinuities and crack opening by enabling a local enrichment of approximation spaces. With the additional degrees of freedom from special enrichment functions, once the failure criteria are fulfilled, cracks are allowed to initiate in local enrichment regions and to propagate based on the energy release criteria without the need for conventional re-meshing. Due to the absence of remeshing requirements, XFEM has become one of the choice methods for modelling fracture of cohesive materials [2-5].

Theoretically, the simplest laboratory testing method for the measurement of tensile strength is the Direct Tension Test (DTT). The method has been extensively implemented in the investigation of the tensile strength of over-consolidated clays, unsaturated soils, and cemented sands. However, the complicated process of specimen preparation is a significant obstacle [6, 7]. Coupled with potential bias when compared with the Brazilian Testing method [8], Tang et al. [9] developed an XFEM model using Abaqus code [10] to simulate crack opening and tension failure in Unconfined

Expansion Testing (UET) in order to analyse both the stress distribution of the test and to examine fracture parameters. UET (as seen in Fig. 1) is a newly designed test that aims at measuring the tensile strength of intermediate geotechnical materials (IGM) such as soft rocks. A cylindrical cavity is drilled along the axis of a cylindrical specimen, then, based on Timoshenko's thick wall cylinder expansion theory [11] the UET method is able to create circumferential, uniformly-distributed tensile stresses around the sample cavity by the inflation of an expandable probe. Therefore, an arbitrary crack path is created when natural weaknesses of the sample approach the material's tensile strength. XFEM simulation results confirm an agreement with theoretical assumptions in both pre-failure stress distribution and tensile strength [9]. As stresses evenly develop inside the geometry, a radial XFEM region must be predefined within the geometry to overcome the computational ambiguity of crack opening when XFEM is specified over the full domain.

Of particular interest in the study of UETs is the impact of material heterogeneity. This can be achieved by interpolating XFEM with material variability and performing probabilistic analyses. Probabilistic analysis of heterogeneous brittle materials has continued to gain significant attention [2, 12, 13]. Understanding of the relationship between heterogeneity and UET test results has two benefits. For materials with known heterogeneity, the method can be applied to determine the test quality and possible error. For unknown heterogeneous materials, engineers can back-estimate the material's heterogeneity by performing a large number of tests.

This paper introduces the existing uniform XFEM simulation of UET but without a predefined fracture zone. Commencing with the theory of discontinuity simulation by XFEM for implementation of UET modelling, comparisons of scenarios with and without the predefined XFEM region are produced. The process of random variable parameter assignment is detailed, followed by XFEM simulation results. With the aforementioned approach, the goal of this research is to allow fracture to form naturally without predefined XFEM zones, by the process of random variable assignment of element parameters. Furthermore, this paper presents the effects of this process on material strength, such that stochastic models incorporating variation of material characteristics can be calibrated to align with observed laboratory UET results, while also producing numerical results to develop conclusions about empirical UET parameter variability.

Fig. 1. UET probe placed within a brown coal specimen, Tang et al. [9]

2. The Extended Finite Element Method Overview

The extended finite element method is an indispensable tool for modern numerical simulation of crack initiation, propagation, and coalescence. Initially developed by Belytschkoand Black [1, 15], XFEM supplements the classic finite element method with local enrichment functions applied to finite element approximation spaces. Alternative existing techniques for fracture simulation include boundary element methods [16, 17], continual re-meshing FEM [18], and mesh-free methods [14, 19]. However, XFEM exhibits a wide range of beneficial attributes; without the enrichment properties of the extended method, conventional FEM requires appreciable mesh refinement in the neighbourhood of discontinuity tips. Discrete crack propagation phenomena are often modelled efficiently with XFEM without the constraint of extensive re-meshing, a crucial property for computationally expensive non-linear systems. XFEM incorporates the added benefit of integrating readily available codes to existing finite element algorithms and framework.

2.1. Theory

In the extended finite element method, the span of functions for the element-free Galerkin method of Fleming, Chu [19] is implemented utilising Partition of Unity (PU) theory developed by Melenk and Babuška [20], and Duarte and Oden [21]. The PU method provides analysis of material behaviour characteristics throughout element geometries, rather than exclusively at element nodes. Consequently, mesh and discontinuity alignments are nonessential. Additional degrees of freedom produce near crack tip nodes by enrichment functions. The displacement approximation u, with the partition of unity enrichment is expressed in Equation 1 [10]

$$\boldsymbol{u}^h = \sum_{i \in I} \boldsymbol{u}_i \phi_i + \sum_{j \in J} \boldsymbol{b}_j \phi_j \, H(x) + \sum_{k \in K} \phi_k \left(\sum_{l=1}^{4} \boldsymbol{c}_k^l F_l(\boldsymbol{x}) \right) \qquad \text{[Eq. 1]}$$

where the first contributing part $\mathbf{u}_i$ corresponds to the classical FEM approximation of the displacement field, ϕ_j is the shape function for the j^{th} node whose support is cut by the crack face (but not the crack tip), $\mathbf{b}_j$ is the crack face j^{th} nodal displacement vector; *H(x)* is the modified Heaviside function (Equation 2), $F_l(x)$ are the elastic asymptotic crack tip functions (Equations 3 - 6); $\mathbf{c}^l_k$ is k^{th} nodal enriched degree of freedom vector of the asymptotic crack tip and ϕ_k is the shape function for the k^{th} node whose support is cut by the crack tip. The nodal displacement term $\mathbf{u}_i$ applies to all nodes, while the Heaviside term contributes only to nodes whose support is cut by the crack interior. The final term of Equation 1 is applied only to the nodes whose support is cut by the crack tip.

$$H(\boldsymbol{x}) = \begin{cases} 1 & \text{if } (\boldsymbol{x} - \boldsymbol{x}^*) \cdot \boldsymbol{m} \geq 0, \\ -1 & \text{otherwise} \end{cases} \qquad \text{[Eq. 2]}$$

where, ***x*** is a Gauss point, ***x**** is the projection of ***x*** onto the crack line, and ***m*** is the unit outward normal to the crack at position ***x****.

$$F_{l=1}(x) = \sqrt{r}\, sin\frac{\theta}{2} \qquad \text{[Eq. 3]}$$

$$F_{l=2}(x) = \sqrt{r}\, cos\frac{\theta}{2} \qquad \text{[Eq. 4]}$$

$$F_{l=3}(x) = \sqrt{r}\, sin\frac{\theta}{2} sin\,\theta \qquad \text{[Eq. 5]}$$

$$F_{l=4}(x) = \sqrt{r}\, cos\frac{\theta}{2} sin\,\theta \qquad \text{[Eq. 6]}$$

Where, (r, θ) form the polar coordinate system with the crack tip at the origin.

2.2. Extended finite element simulations with predefined enrichment zones

The numerical fracture simulations of Tang et al. [9] provides an innovative technique for the modelling of the tensile strength of organic soft rock cored specimens. Utilising the XFEM in Abaqus 6.14 FEM code, Tang et al. [9] produced a quarter annulus shaped membrane (Fig. 2) with spatially homogeneous material properties shown in Table 1. As shown in Fig. 2, a predefined thin enrichment XFEM region is extending radially from a centre cavity. Due to the expectation of stress developing uniformly through the model geometry, crack initiation and propagation are exclusively allowed to develop within the desired XFEM region.

To trigger the crack initiation, the failure criterion was defined by a Maximum Principal Stress Failure Criteria (MPSFC) of 130kPa, suitably modelling failure under tension. Conversely, the deviatoric stress criterion modelled failure in compression, as expected in elements close to the annulus cavity wall, where aperture expansion may cause excessive compression.

In preference to implementing a computationally expensive full three-dimensional model, a thin layer consisting of 3842 eight-node linear brick reduced integration elements (ABAQUS type C3D8R) was deemed a suitable specimen geometry for initial analysis. A thin 3D layer was chosen in preference to a 2D plane-strain model, due to the contact formulation of the inner cavity. Abaqus 3D shell elements (S4R 4-node reduced integration) were chosen due to the number of contact elements, in comparison with the Abaqus beam elements (B31) of 2D plane-strain simulation.

Boundary conditions illustrate side 1 as fixed in the Y direction, side 2 fixed in the X direction, and sides 3 and 4 fixed in the Z direction (Fig. 2). Isotropic cylindrical pressure applied to side 5 simulated the expansion of the internal cavity, providing conditions to trigger fracture initiation. The full dimensions of the UET sample and the quarter annulus considered for modelling are given in Fig. 3**.**

Table 1. Input parameters of initial quarter annulus model

Tensile strength (kPa)	Poisson's ratio	Critical energy release rate (Pa m)	Elastic modulus (MPa)	Friction angle (degrees)	Cohesion (kPa)
130	0.22	2.357	19	20	150

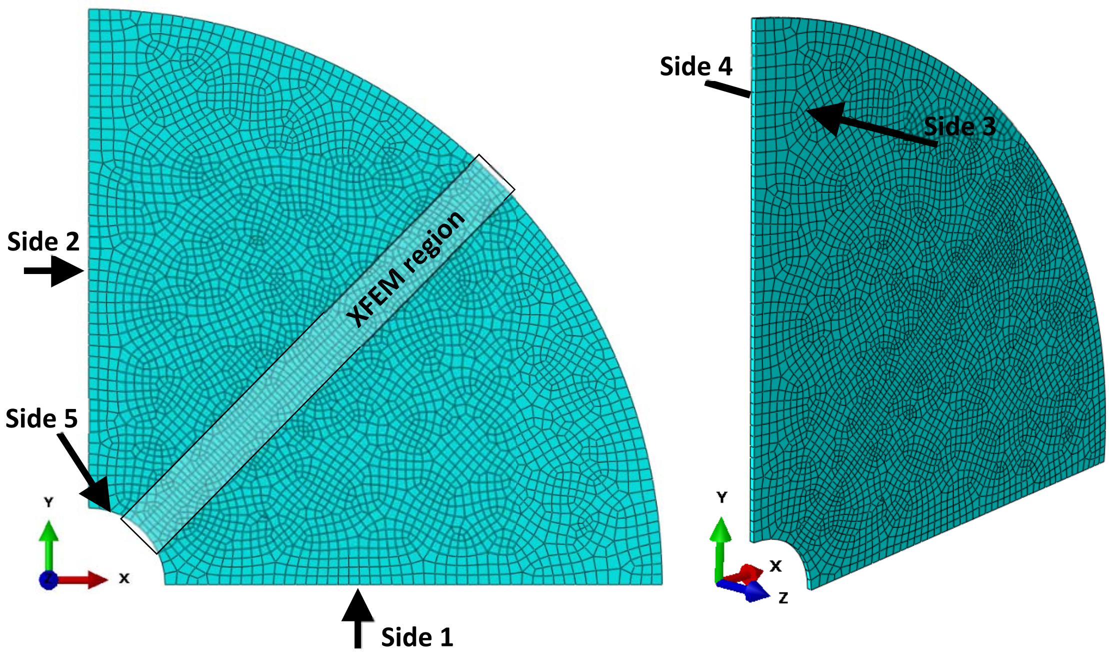

Fig. 2. XFEM geometry of *Tang et al.* [9]

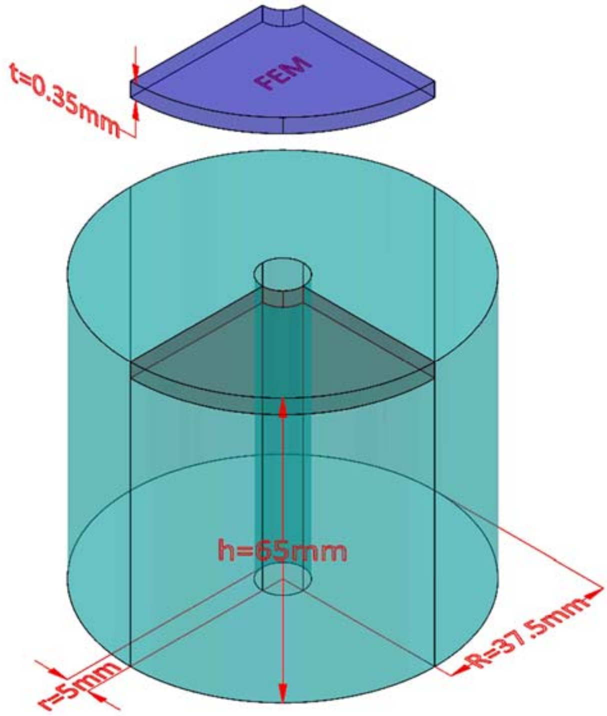

Fig. 3. Quarter annulus of UET sample used for FEM modelling

2.3. Heterogeneous XFEM model without predefined enrichment zone

The model described above constitutes a powerful technique for the simulation of cracked specimens mimicking unconfined expansion tests. However, the prescription of a defined failure region (XFEM region in Fig. 2) represents an unrealistic system. In the paper presented, methods permit solution dependent fracture paths to develop, without the need to predefine the failure region.

In the absence of heterogeneous material characteristics in numerical simulation of isotropic loading scenarios such as UET, homogeneous parameters of elastic modulus and maximum tensile strength are allocated to all specimen elements. Hence, fractures are unable to differentiate strong and weak zones and propagate uniformly, making numerous fractures developing radially from the inner cavity (Side 5). This method of homogenous crack initiation and propagation is not only unrealistic but also causes the solution to fail after a few unconverged iteration (see Fig. 4). To solve this limitation, material variability should be introduced in numerical modelling. The maximum principal stress crack initiation criteria which is available in Abaqus enhanced with the addition of heterogeneous strength parameters allows cracks to initiate naturally, meaning no initial fractures were designed within the Finite Element geometry. Instead, cracks form without predefined orientations, locations and dimensions, with crack characteristics determined by the cavity expansion applied to the unique instance of the of material's maximum principal stresses. Due to the energy release rate and the material strength values, cracks propagate orthogonal to the orientation of the internal cavity.

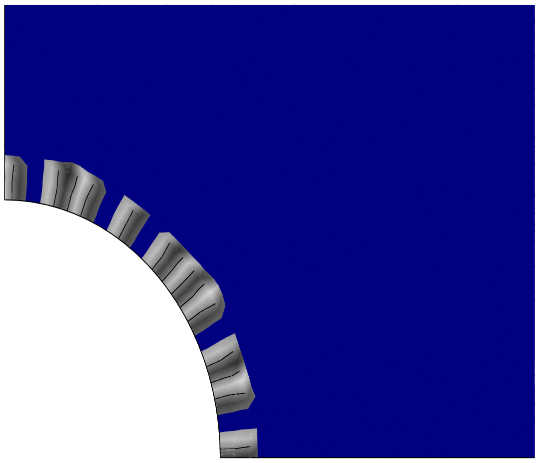

Fig. 4. Multiple cavity fractures caused by material homogeneity

3. Assign material variation into XFEM

3.1. Definition of model variability

It is widely accepted that computational methods aid the construction and analysis of engineering systems ranging from the nano-scale to the macro-scale. Inherent material uncertainties and their influence on system behaviour have led to an increase in stochastic methods applied to geotechnical problems of high complexity. Numerical simulations containing stochastic and heterogeneous soil models are gaining attention in broad range of geotechnical engineering fields, from slope stability analysis [22, 23] to discrete fracture networks [24]. Heterogeneous characteristics may be applied to include Poisson's ratio, elastic modulus, yield stress, methods of loading, etc. Heterogeneities are often generated by means of statistics and probability theory, with resulting behaviour that cannot be achieved by classical deterministic approaches.

3.2. Numerical Definition of Material Variation

Due to the Central Limit Theorem (CLT), sufficiently large random samples of a population of finite variance, produce sample means approximately equal to the mean of the population. Furthermore, sample means will follow an approximately Gaussian distribution, with sample variances mirroring the population variance. Although uncertainties in soil mechanics may follow non-Gaussian distributions, stationary Gaussian random fields are routinely assumed for the sake of simplicity and due to a lack of knowledge regarding experimental data. This paper concentrates exclusively on the normal (Gaussian) distribution for the variation of element maximum principal stress failure criteria and element elastic modulus. The fluctuations in these properties suggest an approach for the production of spatial variation in crack initiation and propagation. As the objective of this research is to naturally produce fracture by material strength parameter variation, the analysis of non-Gaussian distributions is deemed beyond the scope of this paper. Spatially random variables without a spatial correlation length have been implemented in this research, as spatial correlation parameters are not required to produce the goal of fracture initiation.

Material properties are varied as a percentage of their mean value (Fig. 5). As maximum principal stress and elastic modulus variables permit only non-zero values, random variables outside the range of $[0, 2\mu]$ were rejected and given random normal values within the permissible domain. This process produced a truncated Gaussian distribution free from skew.

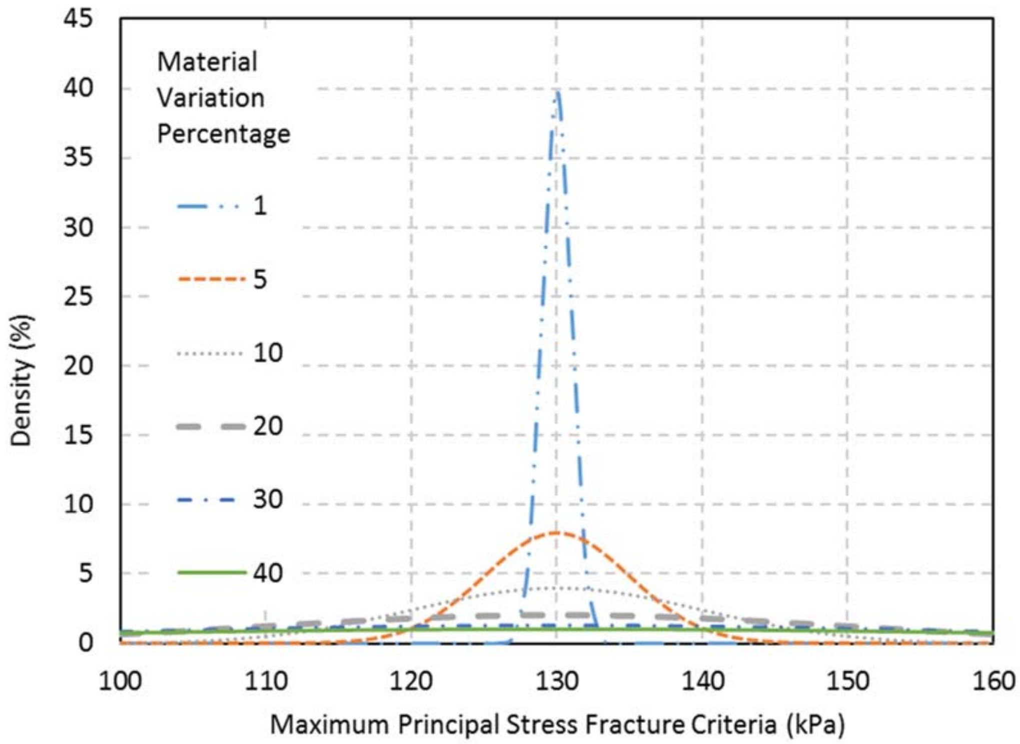

Fig. 5. Distribution of maximum allowable principal stress in tension (fracture initiation criteria)

3.3. Simulation methodology

The proposed method is specified by the following procedure and in Fig. 6.

(1) Meshing the domain with Abaqus CAE to create an input (inp) file. A fine mesh is required to ensure crack paths are modelled with satisfactory resolution;

(2) Generating normally distributed tensile strength and elastic modulus parameters for each finite element using in-house Python scripts;

(3) Assigning material element properties to finite elements, indexed within input files generated by Abaqus;

(4) Implementing Abaqus standard solver, running cavity expansion simulation (UET) and producing pressure-volume curves and Abaqus ODB files;

(5) Exporting pressure-volume data to a spreadsheet;

(6) Repeating steps (2-5) for a sufficient number of random initial configurations, as required by the Monte Carlo simulation method. This process is automated by the creation of a batch file;

(7) Determining cavity strength parameters immediately prior to specimen failure;

(8) Conducting statistical analysis using the statistical package R [27].

This procedure is implemented to produce spatially dependent crack initiation and propagation, unachievable in spatially uniform and homogenous materials.

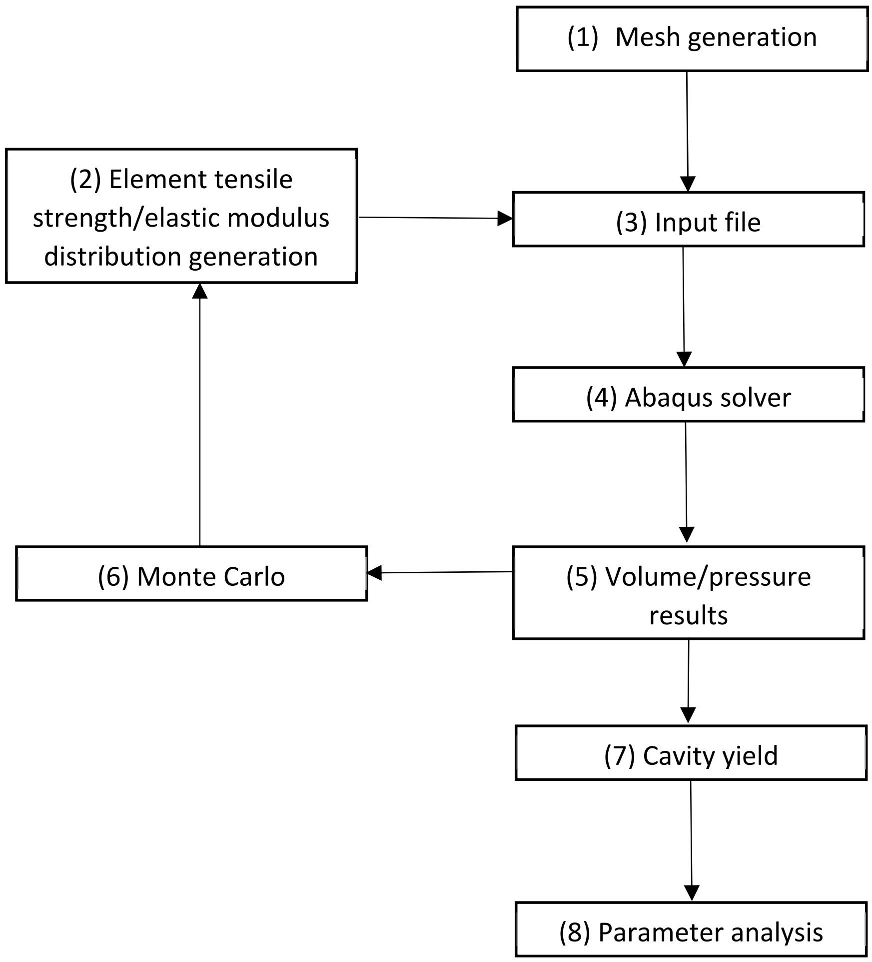

Fig. 6. Analysis procedure flowchart

To determine the impact of fluctuating tensile strength and elastic modulus, a one-factor-at-a-time sensitivity analysis was conducted consisting of the variation of four parameters:

1) Impact of mean tensile strength fracture initiation criteria

Element Maximum Principal Stress Failure Criteria (MPSFC) values for XFEM crack initiation were generated with distribution means of 104, 117 and 130kPa, each with a spread of 20% of the mean strength value. The spread is expressed such that three standard deviations each side of the mean contains stress values within 20% of the mean principal stress. The variation of cavity pressure at initial fracture is then determined in terms of mean and percentage spread of yield pressure mean.

2) Impact of tensile strength fracture initiation criteria spread

Element MPSFC values are generated with a mean of 130kPa and a spread of 1, 5, 10, 20, 25, 30 and 40 percent of the MPSFC mean. Similarly, cavity yield pressure mean and percentage spreads are determined.

3) Impact of elastic modulus distribution mean

Elemental elastic modulus values are generated with a mean of 15.2, 19 and 22.8MPa and 20% mean elastic modulus variation. From the cavity pressure-strain curve, the elastic modulus can be determined from the linear component of the pressure versus change volumetric strain, as shown by Wood [25] (Equation 7). This is then used to calculate a mean output elastic modulus for the model from Hooke's law (Equation 8). Output elastic modulus mean and percentage material spreads are then determined.

$$G = V_0 \frac{dp}{dV} \qquad \text{[Eq. 7]}$$

$$E = 2G(1 + \nu) \qquad \text{[Eq. 7]}$$

where, G is shear modulus, V_0 is initial volume of the cavity, E is elastic modulus, and ν is Poisson's ratio of the UET sample.

4) Impact of elastic modulus distribution spread

Elemental elastic modulus values are generated with a mean of 1.9MPa and spreads of 1, 10, 20 and 30%. The yield elastic modulus mean and percentage material spreads are then determined using the same method as in procedure (3) detailed above.

4. Results

Examples of element variation are shown in Fig. 7. Four instances of crack propagation of the elemental MPSFC with Gaussian distribution (μ = 130000, σ = 4333.33) are presented in Fig. 8 with contour fields signifying displacement magnitude. As expected, element heterogeneity of fracture criteria allows crack paths to develop nonuniformly, radially extending from the interior cavity.

Although the samples in 7(a) and (c) produced a solitary fracture, 7(b) and (d) indicate that multiple fractures are capable of forming.

As the goal of producing spatially nonuniform cracks has been achieved, analysis of the strength properties of heterogeneously distributed element characteristics is investigated using the methods detailed above.

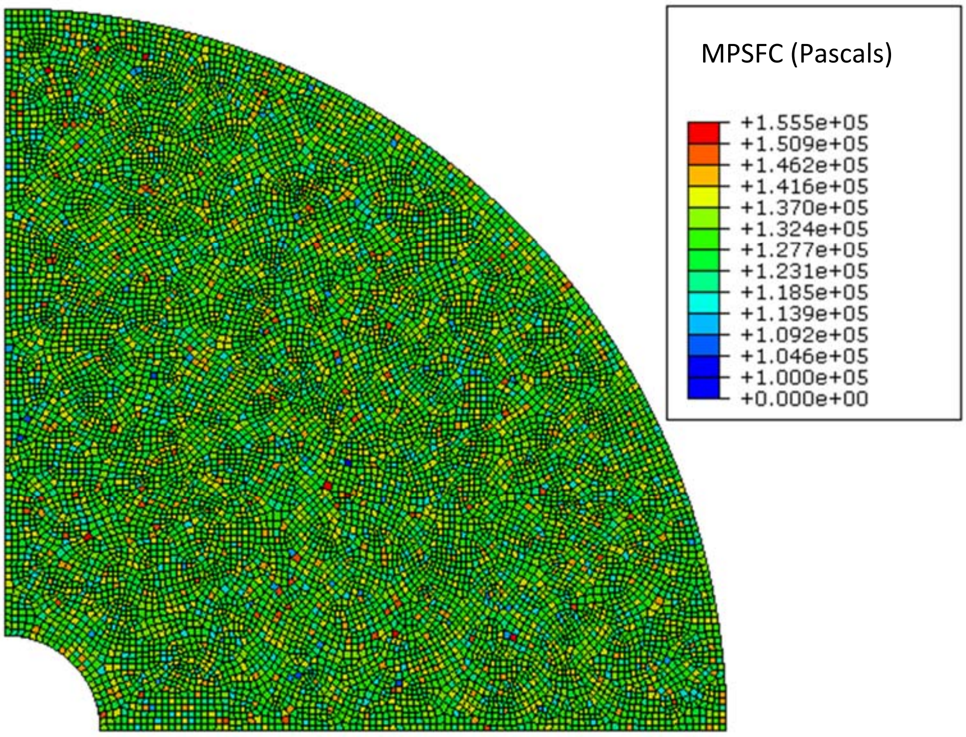

Fig. 7. Specimens with heterogeneous maximum principal strength fracture initiation criteria

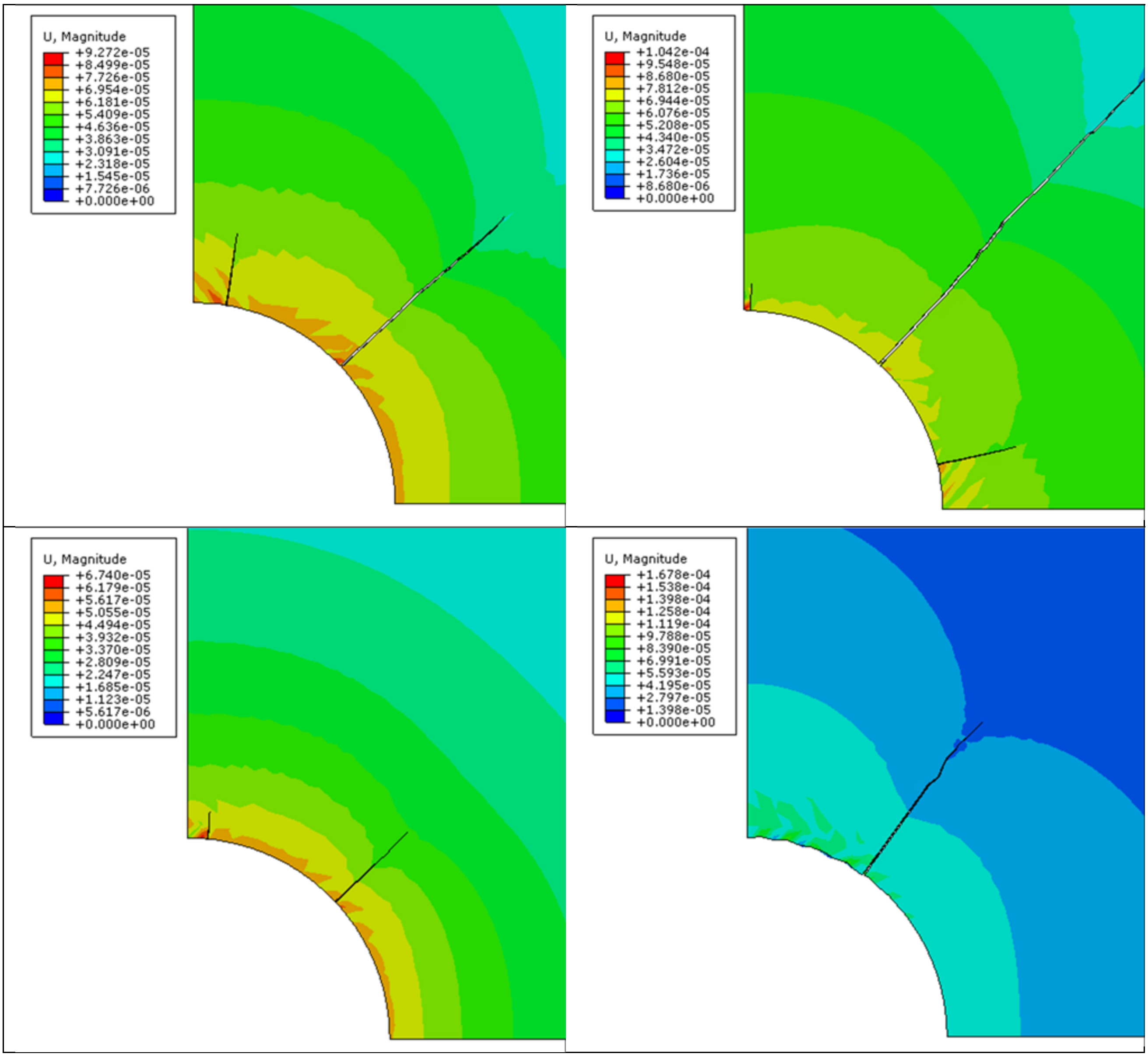

Fig. 8. Four crack propagation instances (μ = 130000, σ = 4333.33)

4.1. Impact of mean tensile strength fracture initiation criteria

When assessing the impact of tensile strength initiation criteria variation, (Table 2, Fig. 9 and Fig. 10) suggests Gaussian MPSFC distributions with 20% spread have the impact of producing a material that will fail at a cavity pressure (primary failure) slightly lower than the mean MPSFC (between 2% and 3% lower). This is to be expected as crack paths will propagate through weak zones while avoiding regions of high tensile strength. Thus cavity pressures less than the mean MPSFC cause the sample to fracture.

Similarly, yield cavity pressures spreads are smaller than the MPSFC variation of 20% for each of the mean MPSFC values tested. While the percentage differences between mean MPSFC and cavity yield pressure seem mostly unaffected by MPSFC means, the percentage change in spread parameters is more varied. Of particular interest is the narrowing of the distribution of yield cavity pressures, compared with MPFSC variation. This suggests that widely varying MPSFC elements produce a much narrower band of yield pressures (observed between 38% and 47% less). As the initial difference of 30μm between the cavity and probe radius observed in laboratory testing was not considered for this simulation, the XFEM results are plotted from $dv/dv_0 = 0.013$ (Fig. 9). The whisker plot of Fig. 10 details similar variation for each distribution of MPSFC with increasing mean strength.

Table 2. Variation of mean tensile strength fracture initiation criteria

Mean elemental MPSFC (kPa)	Mean cavity yield pressure (kPa)	Percentage change in mean parameters	MPSFC variation (%)	Yield cavity pressure variation (%)	Percentage change in spread parameters
104	100.8	-3.07692	20	11.56	-42.2
117	113.1	-3.33333	20	12.38	-38.1
130	127.2	-2.15385	20	10.51	-47.45

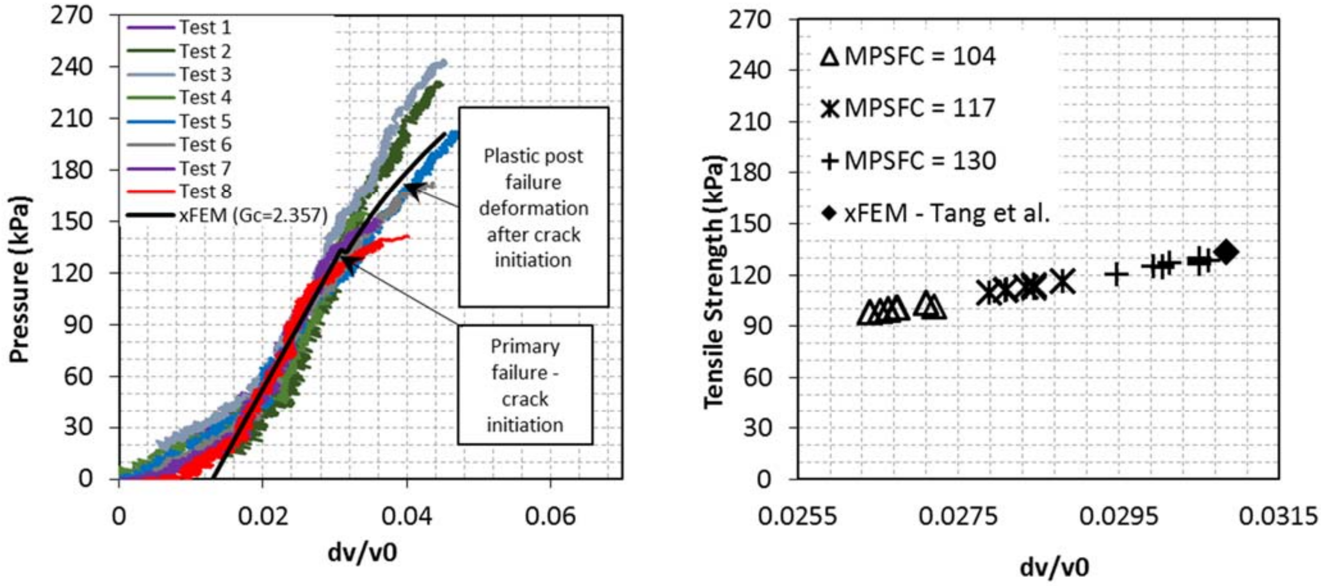

Fig. 9. Variation of yield pressures (primary failure) compared with experimental results produced by Tang et al. [9]

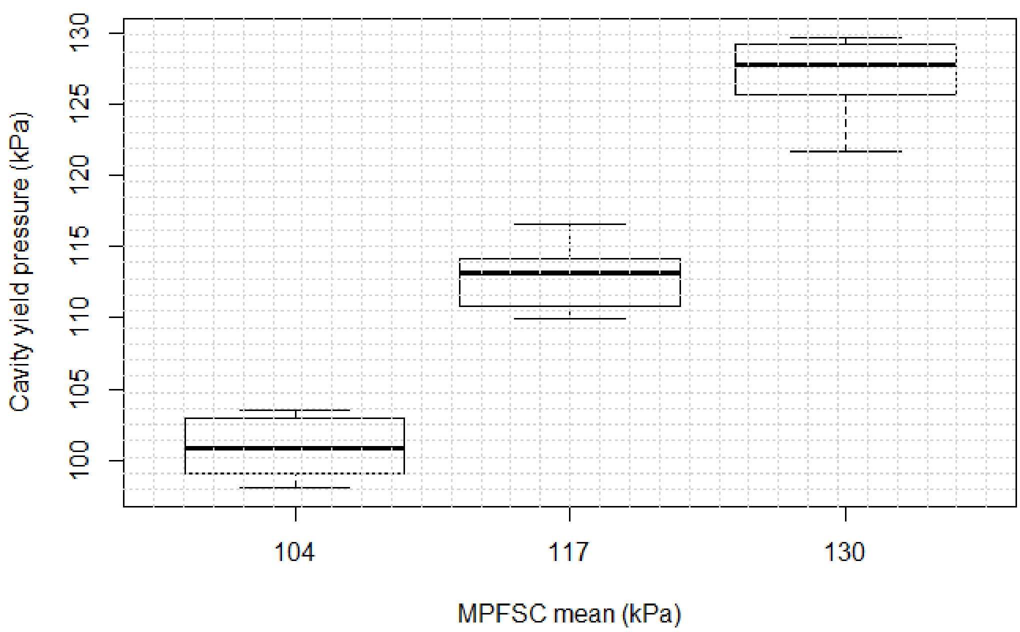

Fig. 10. Whisker plots of mean tensile strength fracture initiation criteria

4.2. Impact of tensile strength fracture initiation criteria spread

The impact of the distribution spread for a fixed mean MPSFC of 130kPa is detailed in Table 3. As expected, increased MPSFC element variation produces a wider range of cavity yield pressures, as shown in Fig. 12. It is immediately obvious that variation of input MPSFC parameters does not produce equal yield cavity pressure spreads. For low MPSFC spreads, the material requires cavity pressures above the MPSFC mean to initiate fracture. Further increasing the spread weakens the material such that cavity pressures well below the mean tensile strength initiation criteria produce cracks.

It is noted MPSFC spread variation has a much greater impact on cavity yield pressure spread than mean cavity yield pressure, especially for small spread values. For small input spreads, the cavity pressure spread increases above the input spread, before drastically narrowing. Several outliers are observed however, their removal impact is deemed minimal.

To produce models for tensile strength of Loy Yang brown coal between 110kPa and 130kPa as reported by Tolooiyan, Mackay [26], a MPSFC mean of 130kPa with a spread of 40% (Table 3) are proposed. These parameters produce a material with a tensile strength of 119.3kPa and spread between 110.64kPa and 127.96kPa. This range lies within the primary failure zone detailed by Tang et al. [9] for Yallourn brown coal.

Table 3. Tensile strength fracture initiaion criteria spread

Mean elemental MPSFC (kPa)	Mean yield cavity pressure (kPa)	Percentage change in mean parameters	MPSFC spread (%)	Cavity yield pressure spread (%)	Percentage change in spread parameters
130	132.5	1.92	1	3.44	244
130	132.2	1.69	5	5.25	5
130	130.4	0.31	10	7.42	-25.8
130	127.2	-2.15	20	10.51	-47.5
130	123.0	-5.38	25	17.74	-29.0
130	121.4	-6.62	30	21.09	-29.7
130	119.3	-8.23	40	17.32	-56.7

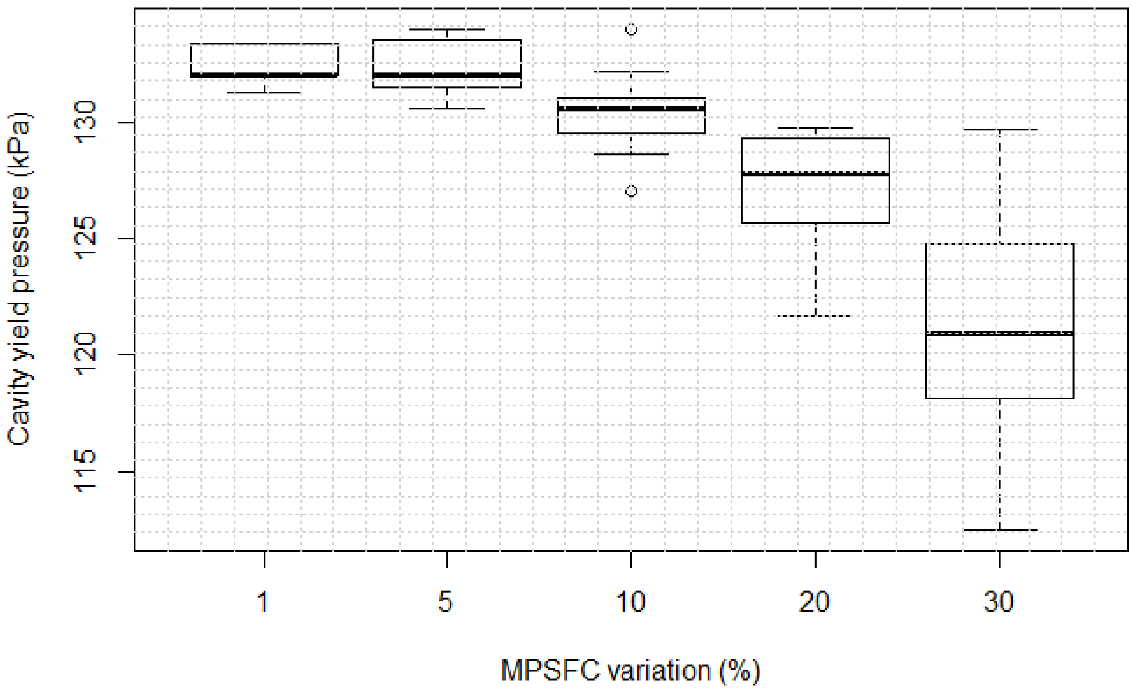

Fig. 12. Whisker plots of tensile strength fracture initiaion criteria spread

4.3. Impact of elastic modulus distribution mean

Investigation of varying element mean elastic modulus values (Fig. 13 and Table 4) indicate that the element mean elastic modulus does not substantially impact the output elastic modulus variation. It is noted in the whisker plot of Fig. 13 that the mean output elastic modulus is minutely diminished compared to the elemental elastic modulus mean. Despite a variation of 20% on the element elastic modulus spread, the output elastic modulus spread is particularly narrow (less than 1.5%) compared with MPSFC variation (Table 2). It is noteworthy that the effects of element elastic modulus variation related to output elastic modulus mean and deviation are considered negligible.

Table 4. Elastic modulus distribution mean values

Mean elemental elastic modulus (MPa)	Mean output elastic modulus (MPa)	Percentage change in mean elastic modulus	Elastic modulus spread (%)	Elastic modulus spread (%)	Percentage change in elastic modulus spread
15.2	15.06	-0.95	20	1.21	-93.95
19	18.91	-0.47	20	0.95	-95.25
22.8	22.78	-0.07	20	0.71	-96.45

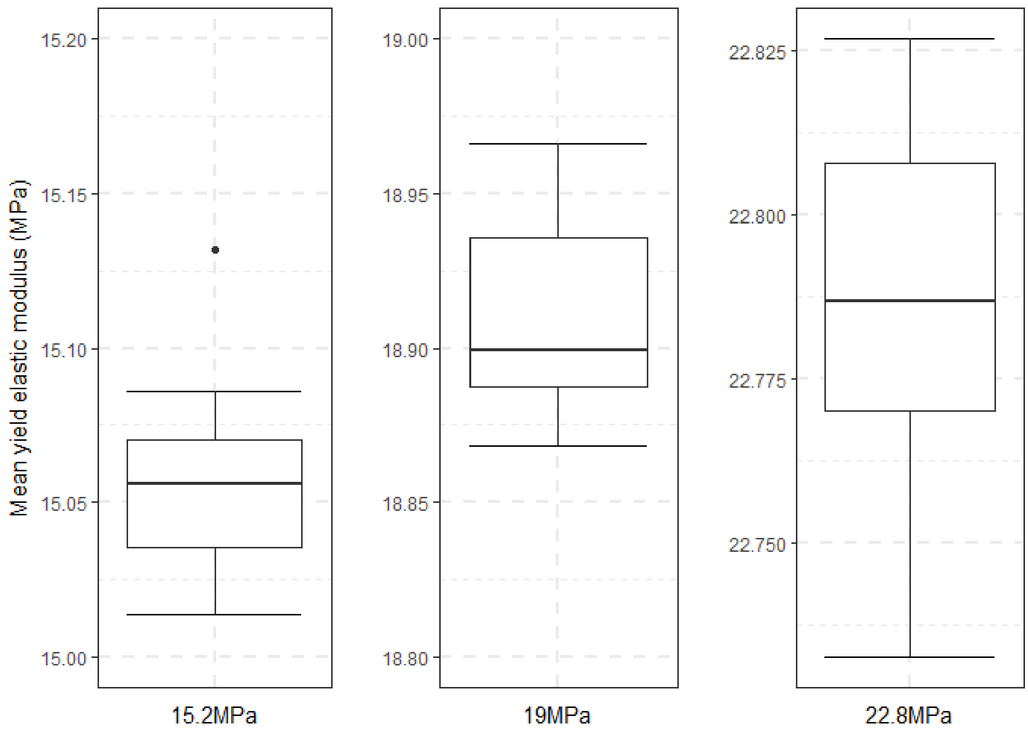

Fig. 13. Whisker plots of elastic modulus distribution mean values

4.4. Impact of elastic modulus distribution spread

Variation of element elastic modulus spread (Table 5 and Fig. 14) shows little impact on mean output elastic modulus values while output elastic modulus spreads remain close to constant. This suggests that probabilistic variation of elastic modulus values is an unnecessary parameter for the variation of output elastic modulus.

Table 5. Impact of elastic modulus distribution spread

Mean elemental elastic modulus (MPa)	Mean output elastic modulus (MPa)	Percentage change in mean elastic modulus	Element elastic modulus spread (%)	Output elastic modulus spread (%)	Percentage change in elastic modulus spread
19	18.91	-0.47	1	0.063026	-93.70
19	18.91	-0.47	10	0.58813	-94.12
19	18.91	-0.47	20	1.050684	-94.75
19	18.89	-0.58	30	0.957721	-96.81

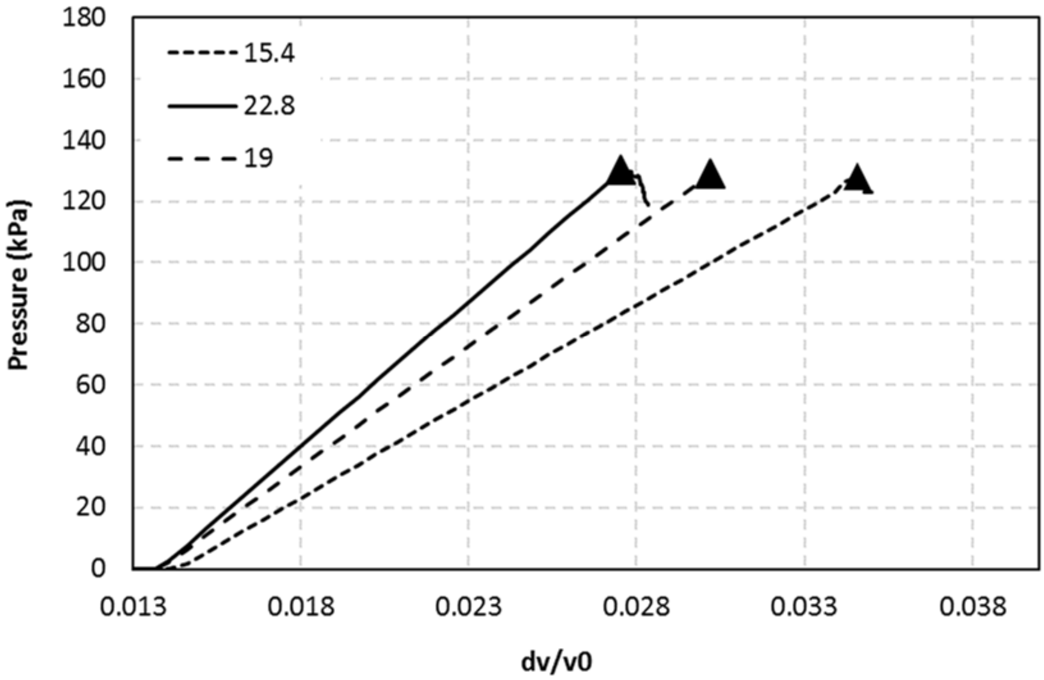

Fig. 14. Primary failure locations

5. Discussion and conclusion

The simulations described were designed to mimic the uncertainty and variation of strength inherent in specimens of Victorian brown coal as a non-textbook geotechnical material, by the assignment of Gaussian random variables to individual finite elements. Four sets of experiments were performed to determine the sensitivity of heterogeneous XFEM fracture to the distributed parameters of maximum principal stress failure criteria and elastic modulus. Of particular interest was the negligible impact of elastic modulus variation played on failure characteristics. Parameters were determined to accurately simulate brown coal specimen characteristics in alignment with previous test results.

The approach of varying element properties by random variable sampling for extended finite elements lends itself to expanded analysis of full three-dimensional models given sufficient computational resources. The technique accommodates the future study of a wider range of varied model parameters and random variable distributions commonly used in soil mechanics. The addition of spatial correlation length scales provide a supplementary layer of complexity for future implementation.

The results presented in this paper propose that probabilistic distributions of fracture initiation criteria can be applied to XFEM elements to allow fracture initiation and propagation with comparable behaviour to UET testing of laboratory specimens, without the requirement of predefined failure zones. The simulations have demonstrated the impact of heterogeneity in maximum principal stress failure criteria and elastic modulus for the understanding of fracture mechanics in brown coal and intermediate geotechnical material.

Acknowledgements

Financial support for this research has been provided by Earth Resources Regulation of the Victorian State Government Department of Economic Development, Jobs, Transport and Resources. The authors would like to thank Mr. Wayne Powrie, who prepared the equipment and specimens for this research. The assistance of Energy Australia is also acknowledged for their support and help with sample collection. The first author is funded by the Australian Government Research Training Program (RTP) and the GHERG scholarship programme and the second author is funded by the GHERG scholarship programme

References

[1] Belytschko T, Black T. Elastic crack growth in finite elements with minimal remeshing. International Journal for Numerical Methods in Engineering. 1999;45(5):601-20.

[2] Liu H, Alonso-Marroquin F, Williams D. Three-dimensional modelling of the rock breakage process. ISRM Regional Symposium-EUROCK 2009: International Society for Rock Mechanics, 2009.

[3] Salimzadeh S, Khalili N. A three-phase XFEM model for hydraulic fracturing with cohesive crack propagation. Computers and Geotechnics. 2015;69(82-92.

[4] Xie Y, Cao P, Liu J, Dong L. Influence of crack surface friction on crack initiation and propagation: A numerical investigation based on extended finite element method. Computers and Geotechnics. 2016;74(1-14.

[5] Pogacnik J, Elsworth D, O'Sullivan M, O'Sullivan J. A damage mechanics approach to the simulation of hydraulic fracturing/shearing around a geothermal injection well. Computers and Geotechnics. 2016;71(338-51.

[6] Ajaz A, Parry RHG. Unconfined direct tension test for compacted clays. Journal of Testing and Evaluation. 1974;2(3):163-72.

[7] Lu N, Wu B, Tan Chee P. Tensile Strength Characteristics of Unsaturated Sands. Journal of Geotechnical and Geoenvironmental Engineering. 2007;133(2):144-54.

[8] Li D, Wong LNY. The Brazilian Disc Test for Rock Mechanics Applications: Review and New Insights. Rock Mechanics and Rock Engineering. 2013;46(2):269-87.

[9] Tang Z, Tolooiyan A, Mackay R. Unconfined Expansion Test (UET) for measuring the tensile strength of organic soft rock. Computers and Geotechnics. 2017;82(54-66.

[10] Systèmes D. Dassault Systèmes, Abaqus. 6.14 ed. Providence (RI, USA) 2014.

[11] Timoshenko S, Woinowsky-Krieger S. Theory of plates and shells: New York, McGraw-Hill, 1959., 1959.

[12] Kolo I, Abu Al-Rub RK, Sousa RL. Computational Modelling of Fracture Propagation in Rocks Using a Coupled Elastic-Plasticity-Damage Model. Mathematical Problems in Engineering. 2016;2016(15.

[13] Su XT, Yang ZJ, Liu GH. Monte Carlo simulation of complex cohesive fracture in random heterogeneous quasi-brittle materials: A 3D study. International Journal of Solids & Structures. 2010;47(17):2336-45.

[14] Belytschko T, Krongauz Y, Organ D, Fleming M, Krysl P. Meshless methods: An overview and recent developments. Computer Methods in Applied Mechanics and Engineering. 1996;139(1-4):3-47.

[15] Moes N, Dolbow J, Belytschko T. A finite element method for crack growth without remeshing. International Journal for Numerical Methods in Engineering. 1999;46(1):131-50.

[16] Saleh AL, Aliabadi MH. Crack growth analysis in concrete using boundary element method. Engineering Fracture Mechanics. 1995;51(4):533-45.

[17] Wendland W, Cruse TA. Boundary Element Analysis in Computational Fracture Mechanics. Mathematics of Computation. 1990;55(192):870.

[18] Swenson DV, Ingraffea AR. Modeling mixed-mode dynamic crack propagation using finite elements: Theory and applications. Computational Mechanics. 1988;3(6):381-97.

[19] Fleming M, Chu YA, Moran B, Belytschko T. Enriched element-free Galerkin methods for singular fields. International Journal for Numerical Methods in Engineering. 1997;40(8):1483-504.

[20] Melenk JM, Babuška I. The partition of unity finite element method: Basic theory and applications. Computer Methods in Applied Mechanics and Engineering. 1996;139(1-4):289-314.

[21] Duarte CA, Oden JT. Hp clouds-an hp meshless method. Numerical methods for partial differential equations. 1996;12(6):673-706.

[22] Griffiths D, Fenton GA. Probabilistic slope stability analysis by finite elements. Journal of Geotechnical and Geoenvironmental Engineering. 2004;130(5):507-18.

[23] Cho SE. Probabilistic assessment of slope stability that considers the spatial variability of soil properties. Journal of geotechnical and geoenvironmental engineering. 2009;136(7):975-84.

[24] Lei Q, Latham J-P, Tsang C-F. The use of discrete fracture networks for modelling coupled geomechanical and hydrological behaviour of fractured rocks. Computers and Geotechnics. 2017;85:151-176.

[25] Wood RJMDM. Mair RJ, Wood DM. Pressuremeter testing: methods and interpretation. 1st Editio ed. London: CIRIA.

[26] Tolooiyan A, Mackay R, Xue J. Measurement of the Tensile Strength of Organic Soft Rock BT - Measurement of the Tensile Strength of Organic Soft Rock. 2014. ASTM Geotechnical Testing Journal, Volume 37, Issue 6

[27] R: A Language and Environment for Statistical Computing. Release 3.4.3, 2017. http://www.R-project.org/